Journal of Fluorescence (2022) 32:2015–2021
https://doi.org/10.1007/s10895-022-03002-4

RESEARCH

A Colormetric and Fluorescence Probe for Highly Specific Cu^{2+} and its Application in Live Cell Imaging

Shujun Ren[1] · Linting Di[1] · Chang-an Ji[1] · Lizhi Gai[1] · Hua Lu[1]

Received: 7 May 2022 / Accepted: 16 June 2022 / Published online: 13 July 2022

Abstract

Fluorescent probes are intriguing material for ion detection. In this study, 4,4-difluoro-4-bora3a,4a-diaza-s-indacene (BODIPY) containing a dipicolylethylenediamine unit was developed as a colorimetric and fluorescence "turn-off" probe for Cu^{2+}. The probe exhibited higher selectivity for Cu^{2+} than other common metal ions with a detection limit of 8.49 μM. With increasing Cu^{2+} concentration, the probe showed a red-shift in the absorption spectrum as well as fluorescence quenching, possibly due to the intramolecular charge transfer effect of the probe–Cu(II) complex. Furthermore, the probe was used for imaging Cu^{2+} in living cells based on confocal fluorescence imaging. The results show that the probe is an effective tool for detection copper ions.

Keywords BODIPY · Copper ions (Cu^{2+}) · Dipicolylethylenediamine · DFT calculation

Introduction

Metal ions play important roles in various important biological and chemical processes, such as electron transfer, oxygen transport, and drug metabolism [1–3]. The misregulation, deficiency, or excess of metal ions is a known contributing factor in some diseases [1]. Thus, the development of novel fluorophores for highly sensitive and selective detection of ions are crucial. Among the heavy metal ions in the human body, Cu^{2+} plays an essential role in the progression of several neurogenerative diseases, such as Parkinson's, Alzheimer's, and Huntington's disease [4–9]. Compared with existing methods for detecting copper ions [10–16], such as inductively coupled plasma mass spectrometry (ICP-MS), X-ray fluorescence microscopy, and nano-secondary ion mass spectrometry (Nano-SIMS), the fluorescence detection method is superior in terms of high optical selectivity and sensitivity, fast response times, and in situ detection. It is noteworthy that the World Health Organization reported a safe upper limit of 31.47 μM of Cu^{2+} ions in drinking water and 100–150 g/dL in blood [17–19]. Hence, designing a fluorescent probe with a detection limit below these upper limits with adequate specificity for copper ion recognition is worthy of in-depth consideration.

Among many fluorophores developed for ion detection, 4,4-difluoro-4-bora3a,4a-diaza-s-indacene (BODIPY) fluorescent dyes have received considerable interest because of their appropriate photophysical properties, such as high photochemical stability, molar absorption coefficient, and fluorescent quantum yield [20–30]. BODIPY dyes have been widely used in diverse organic functional materials, such as labeling reagents, chemosensors, and laser dyes, and have been well investigated for applications such as probes for cations and anions, photosensitizers in photodynamic therapy, and dye-sensitized solar cells [20–30]. However, relatively few fluorescent probes based on BODIPY have been developed for Cu^{2+} detection [31–38], and most of them suffer from interference by zinc ions, or the formed BODIPY-Cu^{2+} complexes are easily affected by sulfide ions. Therefore, the development of BODIPY-based fluorescent probes that can recognize Cu^{2+} ions in mixed media with high selectivity and sensitivity is still necessary.

Shujun Ren and Linting Di are equally contributed to this work.

✉ Lizhi Gai
lizhigai@hznu.edu.cn

✉ Hua Lu
hualu@hznu.edu.cn

[1] College of Material, Chemistry and Chemical Engineering, Key Laboratory of Organosilicon Chemistry and Material Technology, Ministry of Education, Hangzhou Normal University, Hangzhou, Zhejiang 311121, People's Republic of China

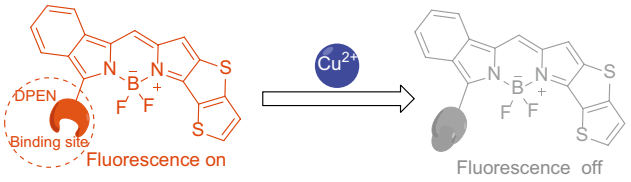

Scheme 1 Designed structures of probe based on benzo[*a*]fused and thieno[3,2-*b*] thiophene-fused BODIPY for detection of Cu^{2+}

Considering this background and following our previous work [39, 40], probe **4** based on nonsymmetric benzo[*a*]-fused and thieno[3,2-*b*]thiophene[*b*]-fused BODIPY dyes was newly prepared (Scheme 1) in this study. This sensor can detect Cu^{2+} in polar mixed solvents with a low detection limit and high sensitivity. In addition, based on the results of high-resolution mass spectrometry (HR-MS), the binding ratio of the sensor and Cu^{2+} was determined to be 1:1. The HOMO and LUMO orbital distributions of the BODIPY–Cu^{2+} complex and dipicolylethylenediamine (DPEN) unit in the chemical sensor were obtained by density functional theory (DFT) calculations for a comprehensive understanding of the recognition mechanism of fluorescence quenching. The probe was used to effectively visualize Cu^{2+} in live cells.

Materials and Methods

Instruments and Reagents

All reagents and solvents were purchased from Energy Chemicals (China) and used without further purification. All reactions were carried out under a dry argon atmosphere by using Schlenk line technique. ^{1}H NMR, ^{13}C NMR and ^{19}F NMR spectra were recorded on a Bruker DRX 500 spectrometer and referenced to the residual proton signals of the solvent. HR-MS were recorded on a Bruker Daltonics microTOF-Q II spectrometer. UV–Vis spectra were obtained by a Shimadzu UV-1800 spectrophotometer. Fluorescence spectra of the samples were recorded on a Horiba JobinYvon Fluorolog-3 spectrofluorimeter. All the solvents employed for the spectroscopic measurements were of spectroscopic grade.

Synthesis

The precursors **1–3** were synthesized and provided in supporting information.

Synthesis of Probe 4

Dye **3** (38.9 mg, 0.1 mmol), DPEN (24.2 mg, 0.1 mmol), and K_2CO_3 (110 mg, 0.8 mmol) were dissolved in dichloromethane (25 mL) under argon, the mixture was stirred at 50 ℃ for 1 h. Then, the solvent of the mixture was removed in vacuo and the residue purified by column chromatography over silica gel (petroleum ether/dichloromethane = 4:1) to give a deep red powder **4** (52.3 mg, 88%). ^{1}H NMR (500 MHz, $CDCl_3$) δ/ppm 8.54 (d, J = 4.0 Hz, 2 H), 7.85 (m, 4 H), 7.78 (t, J = 4.0 Hz, 2 H), 7.64 (d, J = 8.0 Hz, 2 H), 7.42 (t, J = 8.0 Hz, 2 H), 7.30 (d, J = 8 Hz, 1 H), 7.16 (t, J = 8.0 Hz, 2 H), 6,98 (s, 1 H), 6.71 (s, 1 H), 4.06 (dd, J = 4.0 Hz, 2 H), 3.97 (s, 4 H), 3.08 (t, J = 4.0 Hz, 2H). ^{13}C NMR (126 MHz, $CDCl_3$) δ/ppm 158.3, 158.1, 158.0, 148.9, 142.1, 138.1, 137.7, 135.0, 132.2, 131.2, 129.8, 127.5, 126.0, 125.5, 125.4, 125.1, 124.1, 122.7, 121.3, 120.6, 107.5, 107.3, 60.6, 51.5, 41.6. ^{19}F NMR (376 MHz, $CDCl_3$) δ/ppm − 145.12 (q, BF_2). HR-MS (ESI) calcd $C_{31}H_{25}BF_2N_6S_2Na$:$[M]^+$ = 617.1541, found $[M]^+$ = 617.1551.

Preparation of Solutions and Spectral Measurements

A stock solution of probe **4** (1.0 mM) was prepared in CH_3CN. The tested sample solutions of **4** (1 μM) for analysis were prepared by adding 10 μL of the stock solution into the 2 mL of CH_3CN/Water (90:10, v/v), during the titration experiments, a 2 mL solution of **4** was poured into a quartz optical cell with a 1 cm optical path length and the concentrated ion and blank solutions were added using a micropipette. The series of solutions of ions (1 mM for Al^{3+}, Fe^{2+}, Fe^{3+}, Hg^{2+}, Ca^{2+}, Co^{2+}, Cd^{2+}, Mg^{2+}, Ba^{2+}, Mn^{2+}, Ni^{2+}, Zn^{2+}, Na^{+}, K^{+}, Li^{+}, Cu^{+}, and 1 mM, 10 mM for Cu^{2+}) and a blank solution were prepared in deionized water. Spectral data were collected immediately after each addition. For all measurements, the excitation and emission slit widths were set at 5 nm.

Cell Culture and Confocal Imaging

The human NSCLC cell line, PC9 (purchased from the American Type Culture Collection, Manassas, VA, USA) was cultured in DMEM medium supplemented with 10% fetal bovine serum (FBS), 100 μg/mL streptomycin, 100 U/mL penicillin and was maintained at 37 ℃ in a humidified atmosphere containing 5% CO_2. For the fluorescence imaging study, 1×10^5 PC9 cells were seeded on a round cover slides in 24-well plates and cultured for 24 h. The cells were incubated with 5 μM probe **4** (in PBS) for 30 min at 37 ℃, and then washed with PBS for 3 times. The cells were subsequently incubated with 10 μM $CuCl_2$ for 8 min, followed

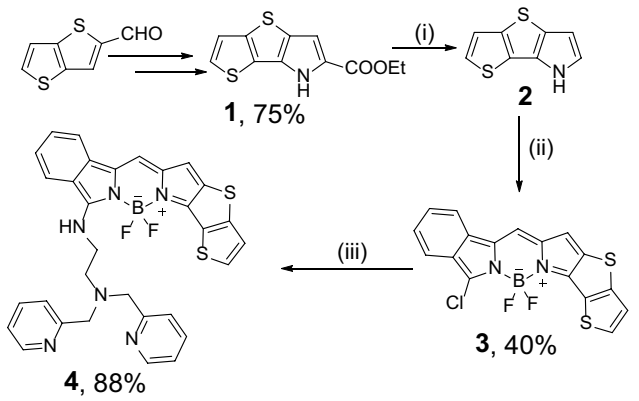

Scheme 2 Synthesis and structure of probe **4**. (**i**) KOH, $(CH_2OH)_2$, reflux, 2 h; (**ii**) 3-chloro-2H-isoindole-1-carbaldehyde, phosphorus oxychloride, 0 ℃, 1 h, triethylamine (10 min) and boron trifluoride etherate, room temperature, 2 h; (**iii**) DPEN, potassium carbonate, and dichloromethane, 36 ℃

by PBS washing for 3 times again. Fluorescence quenching by the intracellular $CuCl_2$ was studied using a confocal fluorescence microscopy (LSM 710 NLO; Carl ZeissMeditec, Dublin, CA, USA).

Computational Details

The ground state and excited state structures of compounds **4** and **4-Cu** were optimized using the density functional theory (DFT) method with B3LYP functional and 6-31G(d, *p*) basis set (LanL2DZ basis for Cu atoms). The LanL2DZ basis set was assigned to the elements of Cu atoms, which guarantees a reasonable balance of the computational cost and the reliability of the results. All the calculations were performed with the Gaussian16 program package [41].

Results and Discussion

Scheme 2 presents the synthesis route of probe **4**. Starting material **1** was prepared in 75% yield according to reported literature [39]. Precursor **2** was synthesized by a reduction reaction performed by refluxing **1** with ethylene glycol in the presence of potassium hydroxide for 2 h. Subsequently, **2** was used for condensation reactions with 3-halogeno-1-formylisoindoles in the presence of $POCl_3$ as a catalyst, followed by treatment with $BF_3{\bullet}OEt_2$ under basic conditions to produce **3** in 40% yield. Target product **4** was obtained by the nucleophilic substitution reactions of **3** and DPEN moieties. We further optimized the reaction conditions. Increasing the reaction temperature further increased the reaction yield of **4** to as high as 88%. The reaction time was longer at this temperature and the yield did not increase, which may be attributed to the fact that basic potassium carbonate affects the stability of the product. The structure of **4** was well characterized by ^{1}H NMR, ^{13}C NMR, ^{19}F NMR, and HR-MS.

To assess the selectivity of probe **4**, its absorption and fluorescence behavior were well investigated upon the addition of various metal ions in CH_3CN/water (90/10, v/v). The main absorption and emission band of probe **4** can be observed at 517 and 585 nm, respectively, in the CH_3CN/water (90/10, v/v) solution (Fig. 1). No distinct changes can be observed in the absorption maximum in the presence of common anions such as Al^{3+}, Fe^{2+}, Fe^{3+}, Hg^{2+}, Ca^{2+}, Co^{2+}, Cd^{2+}, Mg^{2+}, Ba^{2+}, Zn^{2+}, Mn^{2+}, Ni^{2+}, Na^+, K^+, Li^+, Cu^+; however, the maximum band of the absorption and fluorescence spectra decrease upon the addition of Cu^{2+}. The absorption peak at 517 nm decreases gradually, along with the emergence of a new absorption peak at 573 nm, with increasing Cu^{2+} content (Fig. 1c). These changes were accompanied by a change in the color of the solution of **4** from orange to light pink. In addition, the fluorescence emission of probe **4** was quenched completely by Cu^{2+}, along with a color change from yellow to black. The detection limit of Cu^{2+} was calculated to be 8.49 μM based on 3σ/k (Figs. 1d and S1 in ESI) [42, 43]. Therefore, probe **4** is a highly selective and sensitive sensor for Cu^{2+} in the CH_3CN/water (90/10, v/v) solution.

We attempted to fabricate single crystals to better explain the structure–activity relationship between the probe and ions; however, unfortunately, we did not succeed. HR-MS tests were performed on the separated complexes. As shown in Fig. 2, the mass spectrum of **4** in the presence of Cu^{2+} has one peak at $m/z = 656.0895$, which is assigned as $[\mathbf{4} - H^+ + Cu^{2+}]^+$ ($m/z = 656.0866$). These results further confirm that the ratio of probe **4** to Cu^{2+} in the complex was 1:1. To determine the stability of the complex, a solution of **4**–Cu^{2+} was added dropwise to an aqueous solution of sodium sulfide or EDTA (Ethylenediaminetetraacetic acid); no significant change was observed in its absorption spectrum (Fig. S2), indicating that the complexes were very stable. In addition, we tested the effects of light and different pH levels on the probe stability (Fig. S3). Compared to that exhibited by commercial dye rhodamine 6G, probe **4** exhibited better photostability under continuous irradiation with a 525 nm laser for 30 min. No distinct change was observed in the fluorescence emission of the probes at different pH levels. The experimental results show that probe **4** is stable under light illumination and acid/alkali environments, which confirms its excellent application range.

The dark toxicity of probe **4** was first investigated using an MTT (3-[4,5-dimethylthiazol-2-yl]-2,5 diphenyl tetrazolium bromide) assay (Fig. S4). When the probe concentration reached 32 μM, the cell viability was still above 80%, which indicates that probe **4** had little dark toxicity. To demonstrate the practicality of probe **4** for biological

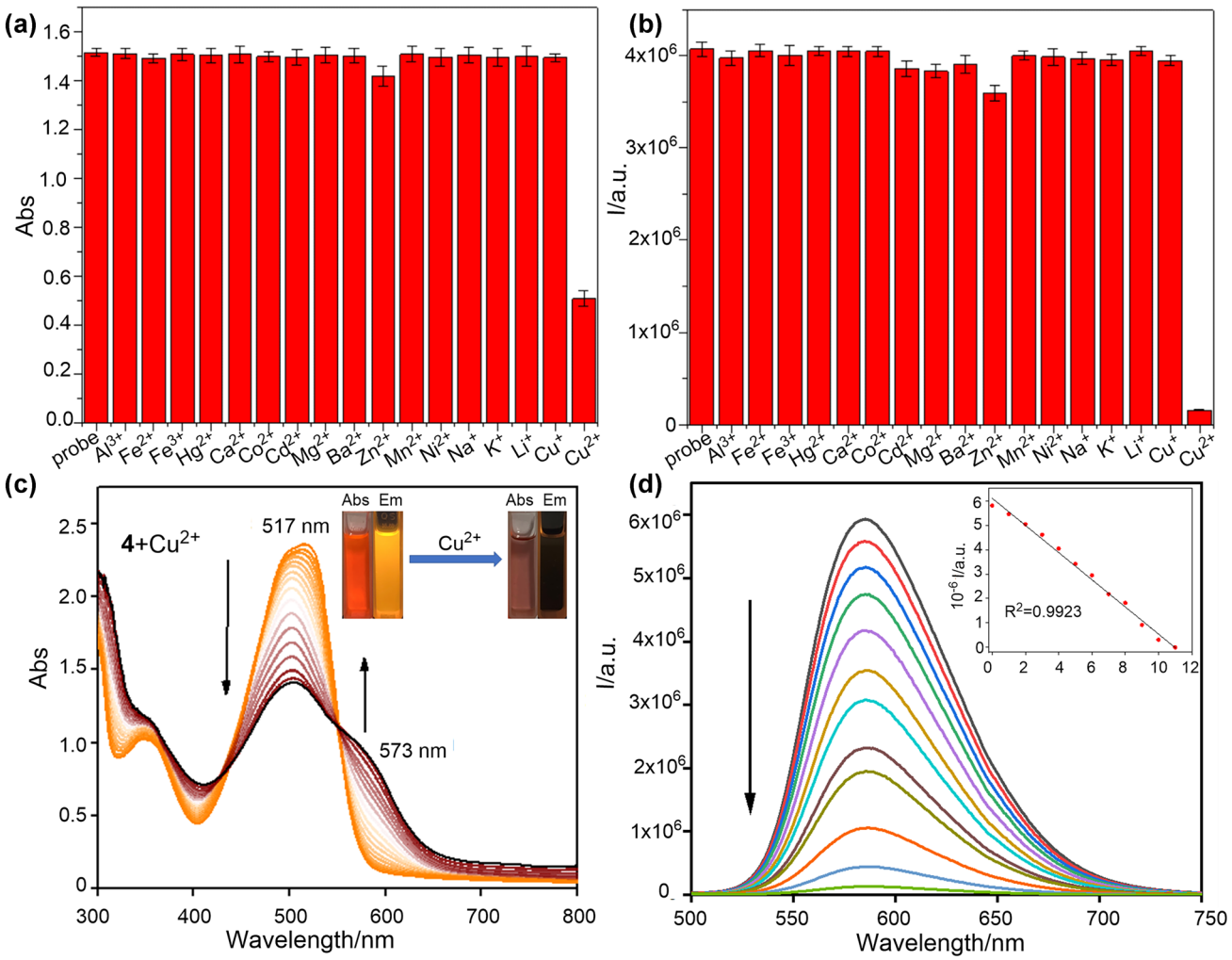

Fig. 1 The maximum absorption spectra (**a**) and emission spectra (**b**) of **4** (10^{-4} M) in CH_3CN/water (90/10) after the addition of 200 equiv. of various anions. (**c**) Absorption spectra of **4** (10^{-5} M) in solution (CH_3CN/water: 90/10) after the addition of Cu^{2+} (1 mM). Inset: photo pictures of **4** (10^{-5} M) before and after adding Cu^{2+} solution. (**d**) Fluorescence spectra of **4** (10^{-5} M) in solution (CH_3CN/water: 90/10) after the addition of Cu^{2+} (1 mM) nm with excitation wavelength at 500 nm. Inset: Plot of emission intensity versus Cu^{2+} concentration ($R^2 = 0.9923$)

applications, we examined the potential applications of **4** for imaging intracellular Cu^{2+} in PC9 cells based on confocal fluorescence imaging experiments. DAPI (4',6-diamidino-2-phenylindole) with blue fluorescence was used to stain the cell nuclei. After staining with probe **4** (5 μM) for 30 min, intracellular red fluorescence was observed (top images in Fig. 3). However, incubation with Cu^{2+} significantly reduced the intracellular red fluorescence intensity, demonstrating that complex **4**–Cu^{2+} was attained in a cellular environment, as shown in Fig. 3 (lower images). These findings indicate that probe **4** can be used for the detection of intracellular Cu^{2+} in living cells.

For an improved understanding of the conformation of BODIPY–Cu^{2+} complexes, the minima structures of **4** and **4**-Cu^{2+} were optimized by DFT calculations using B3LYP in combination with the 6-31G(d, p) basis set for S, B, H, C, N, and F atoms and the LANL2DZ basis set for Cu atoms (Gaussian 16) [41]. As shown in Fig. 4, the Cu atom was coordinated in a tetrahedral geometry by four nitrogen atoms from the DPEN unit with atomic distances of 2.10, 2.22, 2.07, and 2.06 Å. The lowest-energy excitation of **4** was predicted to occur at 507 nm ($f = 0.6$) and to arise primarily from the HOMO → LUMO transitions. However, the lowest-energy excitations of **4**–Cu^{2+} are produced by the HOMO-1 → LUMO transitions with an oscillator strength of 0.13. The HOMO of **4**–Cu^{2+} was almost delocalized in the DPEN–Cu^{2+} unit. Thus, the LUMO is in the BODIPY core containing one nitrogen atom of DPEN. Accordingly, distinct intramolecular charge transfer was observed, which fits well with the experimentally observed

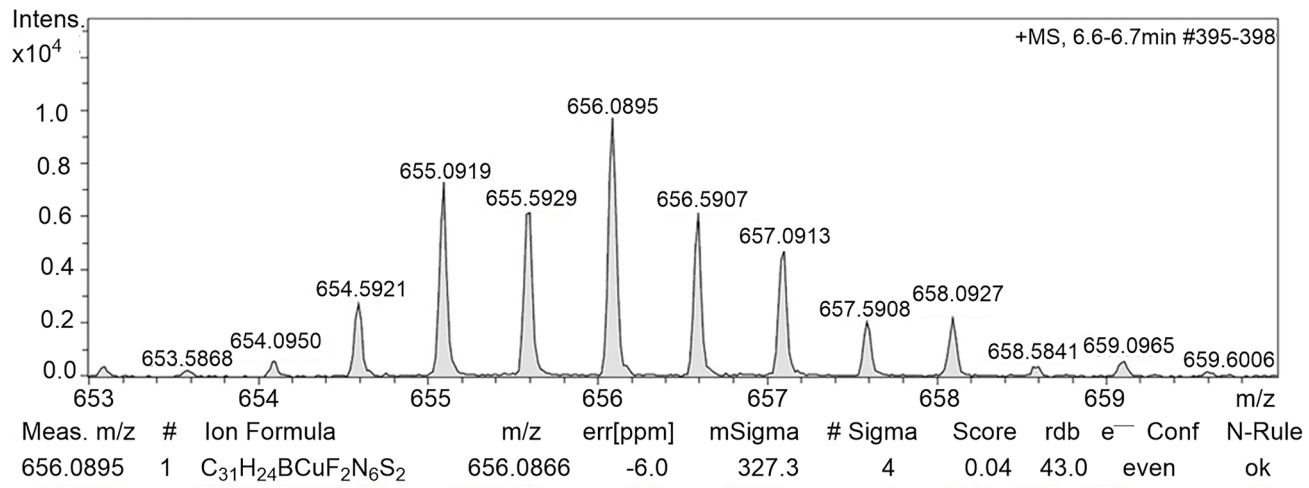

Fig. 2 The HR-MS spectra of **4**-Cu^{2+}

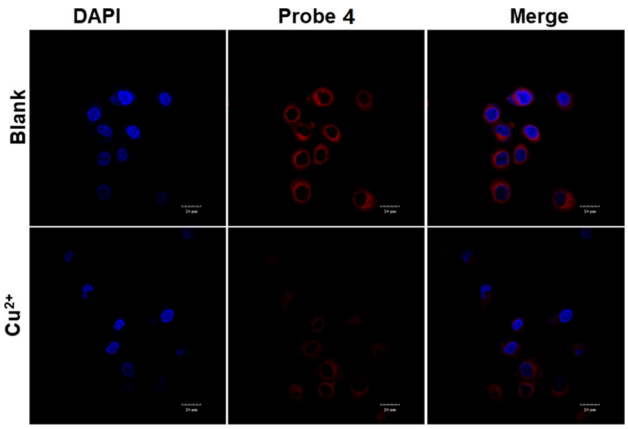

Fig. 3 The confocal fluorescence images of PC9 cells after incubation with probe **4** for 30 min in the absence(top) and (bottom) the presence of Cu^{2+}. Scale bars: 20 μm

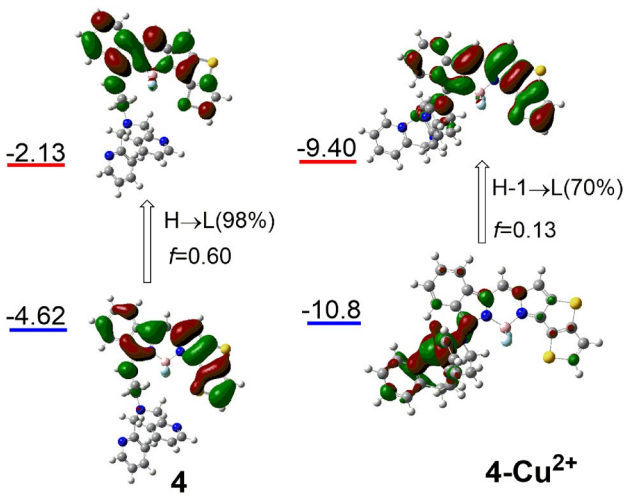

Fig. 4 The optimized molecular structures of probe **4** and **4**-Cu^{2+} complex were calculated by DFT using the B3LYP in combination with 6-31G (d, *p*) basis set for S, B, H, C, N and F atoms and LANL2DZ basis set for Cu atom

"turn-off" fluorescence phenomenon in the emission of **4** before and after complexing with the Cu^{2+} ion.

Conclusions

A probe based on nonsymmetric benzo[*a*]-fused and thieno[3,2-*b*]thiophene[*b*]-fused BODIPY was developed and fully characterized by NMR and HR-MS. Results indicated that probe **4** can be used to detect Cu^{2+} ions with high sensitivity and selectivity, without any interference from other competitive metal ions. HR-MS spectra confirmed the stoichiometry binding of **4** with Cu^{2+} forming a 1:1 complex in the acetonitrile/water (90/10) solution. Imaging experiments confirmed that probe **4** can be applied in the detection of intracellular Cu^{2+} in living cells.

Supplementary Information The online version contains supplementary material available at https://doi.org/10.1007/s10895-022-03002-4.

Author Contribution Shujun Ren: Methodology, Synthesis and resources. Linting Di: Conceptualization investigation, material preparation. Chang-an Ji: Conceptualization, investigation. Lizhi Gai: Review, supervision writing, writing original draft. Hua Lu: Review, supervision.

Funding This work was supported by the National Natural Science Foundation of China (No. 21801057, 21871072). Theoretical calculations were performed at the Computational Center for Molecular Design of Organosilicon Compounds, Hangzhou Normal University.

Data Availability Data generated or analyzed during this study are included in this published article.

Declarations

Ethical Approval This article does not contain any studies with human or animal subjects.

Consent to Participate Not applicable.

Consent for Publication Not applicable.

Conflicts of Interest The authors declare that they have no conflict of interest.

References

1. Gozzelino R, Arosio P (2016) Iron homeostasis in health and disease. Int J Mol Sci 17:130
2. Coleman JE (1992) Zinc proteins: enzymes, storage proteins, transcription factors, and replication proteins. Annu Rev Biochem 61:897–946
3. Daniel KG, Harbach RH, Guida WC, Dou QP (2004) Copper storage diseases: Menkes, Wilsons, and cancer. Front Biosci 9:2652–2662
4. Valentine JS, Hart PJ (2003) Misfolded CuZnSOD and amyotrophic lateral sclerosis. P Natl Acad Sci 100:3617–3622
5. Madsen E, Gitlin JD (2007) Copper and iron disorders of the brain. Annu Rev Neurosci 30:317–337
6. Kim B-E, Nevitt T, Thiele DJ (2008) Mechanisms for copper acquisition, distribution and regulation. Nat Chem Biol 4:176–185
7. Hung YH, Bush AI, Cherny RA (2010) Copper in the brain and Alzheimer's disease. J Biol Inorg Chem 15:61–76
8. Millhauser GL (2004) Copper binding in the prion protein. Acc Chem Res 37:79–85
9. Lee JC, Gray HB, Winkler JR (2008) Copper (II) binding to α-synuclein, the Parkinson's protein. J Am Chem Soc 130:6898–6899
10. Liu Y, Liang P, Guo L (2005) Nanometer titanium dioxide immobilized on silica gel as sorbent for preconcentration of metal ions prior to their determination by inductively coupled plasma atomic emission spectrometry. Talanta 68:25–30
11. Poursaberi T, Hajiagha-Babaei L, Yousefi M, Rouhani S, Shamsipur M, Kargar-Razi M, Moghimi A, Aghabozorg H, Ganjali MR (2001) The Synthesis of a New Thiophene-Derivative Schiff's Base and Its Use in Preparation of Copper-Ion Selective Electrodes. Electroanal 13:1513–1517
12. Gonzales A, Firmino M, Nomura C, Rocha F, Oliveira P, Gaubeur I (2009) Peat as a natural solid-phase for copper preconcentration and determination in a multicommuted flow system coupled to flame atomic absorption spectrometry. Anal Chim Acta 636:198–204
13. Tian Y, Pepelnik R, Fanger H (1990) Multielement analysis of archaic Chinese bronze and antique coins by fast neutron activation analysis. J Radioanal Nucl Chem 139:43–53
14. Rao GPC, Seshaiah K, Rao YK, Wang M (2006) Solid phase extraction of Cd, Cu, and Ni from leafy vegetables and plant leaves using amberlite XAD-2 functionalized with 2-hydroxyacetophenone-thiosemicarbazone (HAPTSC) and determination by inductively coupled plasma atomic emission spectroscopy. J Agric Food Chem 54:2868–2872
15. Jackson KW, Mahmood TM (1994) Atomic absorption, atomic emission, and flame emission spectrometry. Anal Chem 66:252–279
16. Pathirathna P, Yang Y, Forzley K, McElmurry SP, Hashemi P (2012) Fast-scan deposition-stripping voltammetry at carbon-fiber microelectrodes: real-time, subsecond, mercury free measurements of copper. Anal Chem 84:6298–6302
17. Edition F (2011) Guidelines for drinking-water quality. WHO Chronicle 38:104–108
18. Malavolta M (2018) Mocchegiani E. Trace elements and minerals in Health and Longevity: Springer
19. Sharma S, Ghosh KS (2021) Recent advances (2017–20) in the detection of copper ion by using fluorescence sensors working through transfer of photo-induced electron (PET), excited-state intramolecular proton (ESIPT) and Förster resonance energy (FRET). Spectrochim Acta A 254:119610
20. Boens N, Leen V, Dehaen W (2012) Fluorescent indicators based on BODIPY. Chem Soc Rev 41:1130–1172
21. Kowada T, Maeda H, Kikuchi K (2015) BODIPY-based probes for the fluorescence imaging of biomolecules in living cells. Chem Soc Rev 44:4953–4972
22. Lu H, Mack J, Yang Y, Shen Z (2014) Structural modification strategies for the rational design of red/NIR region BODIPYs. Chem Soc Rev 43:4778–4823
23. Yang J, Zhang R, Zhao Y, Tian J, Wang S, Gros CP, Xu H (2021) Red/NIR neutral BODIPY-based fluorescent probes for lighting up mitochondria. Spectrochim Acta A 248:119199
24. Sun Y, Yu X-a, Yang J, Gai L, Tian J, Sui X, Lu H (2021) NIR halogenated thieno [3, 2-b] thiophene fused BODIPYs with photodynamic therapy properties in HeLa cells. Spectrochim Acta A 246:119027
25. Shi H, Zhao F, Chen X, Yang S, Xing J, Chen H, Zhang R, Liu J (2019) Colorimetric and ratiometric sensors derivated from natural building blocks for fluoride ion detection. Tetrahedron Lett 60:151330
26. Liu Z, Jiang Z, Xu C, Chen B, Zhu G (2021) Fluorenyl-difluoroboron-β-diketonates with multi-stimuli fluorescent response behavior and their applications in a thermochromic logic gate device. Dyes Pigm 186:108990
27. Teknikel E, Unaleroglu C (2022) 2, 3, 5, 6-Tetrabromo-8-phenyl BODIPY as a fluorometric and colorimetric probe for amines. J Photochem Photobiol A 422:113549
28. Zhang X-F, Zhang Y, Xu B (2017) Enhance the fluorescence and singlet oxygen generation ability of BODIPY: Modification on the meso-phenyl unit with electron withdrawing groups. J Photochem Photobiol A 349:197–206
29. Wu Q, Wang S, Hao E, Jiao L (2021) Highly selective, colorimetric probes for cyanide ion based on β-formylBODIPY dyes by an unprecedented nucleophilic addition reaction. Spectrochim Acta A 247:119102
30. Kubheka G, Sanusi K, Mack J, Nyokong T (2018) Optical limiting properties of 3, 5-dipyrenylvinyleneBODIPY dyes at 532 nm. Spectrochim Acta A 191:357–364
31. Praikaew P, Roongcharoen T, Charoenpanich A, Kungwan N, Wanichacheva N (2020) Near-IR aza-BODIPY-based probe for the selective simultaneous detection of Cu^{2+} in aqueous buffer solutions and its application in biological samples. J Photochem Photobiol A 400:112641
32. Xia S, Shen J, Wang J, Wang H, Fang M, Zhou H, Tanasova M (2018) Ratiometric fluorescent and colorimetric BODIPY-based sensor for zinc ions in solution and living cells. Sens Actuators B 258:1279–1286
33. Wang J, Xie Y, Wang Z, Song Q (2014) A highly sensitive and selective naked-eye probe for detecting copper ion based on 2, 3-modified Bodipy derivatives. Sens Actuators B 194:149–155
34. Sun R, Wang L, Jiang C, Du Z, Chen S, Wu W (2020) A Highly Efficient BODIPY Based Turn-off Fluorescent Probe for Detecting Cu^{2+}. J Fluoresc 30:883–890
35. More AB, Mula S, Thakare S, Chakraborty S, Ray AK, Sekar N, Chattopadhyay S (2017) An acac-BODIPY dye as a reversible "ON-OFF-ON" fluorescent sensor for Cu2+ and S2-ions based on displacement approach. J Lumin 190:476–484
36. Zhang J, Zhao B, Li C, Zhu X, Qiao R (2014) A BODIPY-based "turn-on" fluorescent and colorimetric sensor for selective

detection of Cu2+ in aqueous media and its application in cell imaging. Sens Actuators B 196:117–122
37. Zeng L, Miller EW, Pralle A, Isacoff EY, Chang CJ (2006) A selective turn-on fluorescent sensor for imaging copper in living cells. J Am Chem Soc 128:10–11
38. Song Y, Tao J, Wang Y, Cai Z, Fang X, Wang S, Xu H (2021) A novel dual-responsive fluorescent probe for the detection of copper (II) and nickel (II) based on BODIPY derivatives. Inorg Chim Acta 516:120099
39. Di L, Yang J, Tang W, Gai L, Zhou Z, Lu H (2020) Nonsymmetric Benzo[a] fused and Thiophene/Thieno [3, 2-b] thiophene [b] fused BODIPYs: Synthesis and Photophysical Properties. J Org Chem 86:601–608
40. Sun Y, Yuan H, Di L, Zhou Z, Gai L, Xiao X, He W, Lu H (2019) Non-symmetric thieno [3, 2-*b*] thiophene-fused BODIPYs: synthesis, spectroscopic properties and providing a functional strategy for NIR probes. Org Chem Front 6:3961–3968
41. Frisch MJ et al (2016) Gaussian 16 Rev. C.01. Wallingford, CT
42. Ogren PJ, Meetze A, Duer WC (2009) The limit of detection in generalized least-squares calibrations: an example using alprazolam liquid chromatography-tandem mass spectrometry data. J Anal Toxicol 33:129–142
43. Montville D, Voigtman E (2003) Statistical properties of limit of detection test statistics. Talanta 59:461–476